

Article

Influence of Zinc Oxide Nanoparticles to Regulate the Antioxidants Enzymes, Some Osmolytes and Agronomic Attributes in *Coriandrum sativum* L. Grown under Water Stress

Muhammad Tajammal Khan ^{1,2} , Shakil Ahmed ¹, Anis Ali Shah ^{3,*} , Adnan Noor Shah ⁴, Mohsin Tanveer ⁵ , Mohamed A. El-Sheikh ^{6,7}  and Manzer H. Siddiqui ⁸

- ¹ Institute of Botany, University of the Punjab Quaid, e Azam Campus, Lahore 54590, Pakistan; tajammalkhan5@gmail.com (M.T.K.); shakil.botany@pu.edu.pk (S.A.)
 - ² Division of Science and Technology, Department of Botany, University of Education, Lahore 5600, Pakistan
 - ³ Department of Botany, University of Narowal, Circular Road, Narowal 51600, Pakistan
 - ⁴ Department of Agricultural Engineering, Khwaja Fareed University of Engineering and Information Technology, Rahim Yar Khan 64200, Pakistan; Adnan.shah@kfueit.edu.pk
 - ⁵ Tasmanian Institute of Agriculture, University of Tasmania, Hobart 7005, Australia; mohsin.tanveer@utas.edu.au
 - ⁶ Botany and Microbiology Department, College of Science, King Saud University, Riyadh 11451, Saudi Arabia; melsheikh@ksu.edu.sa
 - ⁷ Botany & Microbiology Department, Faculty of Science, Damanhour University, Damanhour 22511, Egypt
 - ⁸ Department of Botany and Microbiology, College of Science, King Saud University, Riyadh 2455, Saudi Arabia; mhsiddiqui@ksu.edu.sa
- * Correspondence: anislibot@gmail.com



Citation: Khan, M.T.; Ahmed, S.; Shah, A.A.; Noor Shah, A.; Tanveer, M.; El-Sheikh, M.A.; Siddiqui, M.H. Influence of Zinc Oxide Nanoparticles to Regulate the Antioxidants Enzymes, Some Osmolytes and Agronomic Attributes in *Coriandrum sativum* L. Grown under Water Stress. *Agronomy* **2021**, *11*, 2004. <https://doi.org/10.3390/agronomy11102004>

Academic Editors: Baskaran Stephen Inbaraj and Erika Sabella

Received: 24 August 2021

Accepted: 30 September 2021

Published: 3 October 2021

Publisher's Note: MDPI stays neutral with regard to jurisdictional claims in published maps and institutional affiliations.



Copyright: © 2021 by the authors. Licensee MDPI, Basel, Switzerland. This article is an open access article distributed under the terms and conditions of the Creative Commons Attribution (CC BY) license (<https://creativecommons.org/licenses/by/4.0/>).

Abstract: Climatic variations adversely affect the limited water resources of earth which leads to water stress and influences agricultural production worldwide. Therefore, a novel approach has been introduced to improve the tolerance against water stress in herbaceous nature medicinal plants such as *Coriandrum sativum* by the usage of nanotechnology (foliar applied nanoparticles of ZnOx) coupled with the application of water deficit irrigation. This is an alternative water saving strategy that proved to be efficient to mitigate the *Coriandrum sativum* tolerance against water stress regimes for sustainable yield production through the activation of antioxidant system. Thus, the phenomena of green synthesis have been deployed for the formation of Zinc oxide nanoparticles (ZnOx NPs) from the leaf extract of *Camellia sinensis* L. and zinc acetate dihydrate was used as precursor. Different techniques have been used for the thorough study and confirmation of ZnOx NPs such as UV-vis spectroscopy (UV-vis) X-ray diffraction (XRD), Fourier transform infrared spectroscopy (FTIR), Scanning electron microscopy (SEM) and Elemental dispersive spectroscopy (EDS). The prepared ZnOx NPs exhibit hexagonal wurtzite crystal nature has an average size of 37 nm with high purity. These ZnOx NPs have been further studied for their role in amelioration of water stress tolerance in *Coriandrum sativum* in a pot experiment. Two levels of water stress regimes were employed, IR75 (moderate) and IR50 (Intense) to evaluate the behavior of plant compared to full irrigation (FI). Results showed that under water stress regimes, the 100 ppm of prepared NPs stimulate the antioxidant system by increasing the activity of catalases (CAT), super oxidases (SOD) and ascorbate peroxidase (APX) enzymes and found the maximum at IR50, while the concentration of malondialdehyde (MDA) decreased due to increase in activity of antioxidative enzymes. Furthermore, chlorophyll content and amount of proline also enhanced by the foliar application of prepared ZnOx NPs under moderate water stress (IR75). The results suggested that all the investigated agronomic attributes significantly increased, including plant biomass and economic yield (EY), compared to non-treated ZnOx NPs plants, except for the number of primary branches and LAI. Further, the 100 ppm of prepared ZnOx NPs have great potential to improve water stress tolerance in *Coriandrum sativum* by improving the antioxidant enzymes activity that enhance agronomic attributes for high crop productivity that require further research at transcriptomic and genomic level.

Keywords: antioxidant; biomass; coriander; drought; growth; economic yield; harvest index; leaf area index; NPs

1. Introduction

Agricultural production is directly dependent upon climatic variation, which includes winds, temperature, patterns of precipitation, snowfall and oceans currents. These climatic changes can adversely affect the health and growth of the plant, yield per hectare, cropping system and overall production of crop. Climatic variation exhibits weather extravagances, comprising of droughts (water stress) that affect several aspects such as health, water resources and agriculture. According to researchers, the influence of climatic fluctuations on agriculture has been studied extensively, but these studies did not focus on adaptive modifications that can enhance cropping practices to fight against adverse effect of water stress on yield of crop [1–3].

In addition, population is enlarging day by day, which greatly affects by water stress regardless of other climatic variations. Therefore, there is more demand for water in developing countries. The global scenario of water is in critical figures according to the report of UNICEF 2021 [4]. The consumption of water is increasing from 20% to 30% each year. Further, 70% percent of the earth water is being consumed in the agricultural sector, which is one of the causes of water scarcity due to inefficient usage. According to an estimation, 40% of agricultural production and yield is based on irrigation. However, the growing population is one of the causes to increase in food consumption, which expands the irrigated area by eight times in the past 100 years and ultimately leads to drought conditions [4,5]. These prevailing circumstances will increase the water scarcity and food security risk that badly affect the world economy on a larger scale. To overcome the water shortages in the future and ensure food security, many efforts have been made in agriculture sector to fulfil the global demands. In this context, input of innovative environmental techniques that do not require substantial expenditure are important to increase the biomass production and yield of crops under water stress situations [6]. Therefore, we should reduce the conventional agriculture approaches and use water efficient strategies such as deficit irrigation to mitigate the adverse impacts of water scarcity. Moreover, the usage of growth regulators and nanotechnology to enhance the development and growth of plants, ameliorate water stress tolerance and reduce negative impact on crop yield to increase food production are in trend [7].

In relation to the above context, water scarcity has forced many farmers to avoid cultivating a valuable herbaceous crop, *Coriandrum sativum*, which is susceptible to water stress. No vegetable crop at present can match *Coriandrum sativum* in terms of its current market value. This is one of the oldest herbs used in culinary as well as medical purposes for more than 3000 years. *Coriandrum sativum* is the member of Apiaceae (Umbelliferae) family. It is a native plant of the Mediterranean region and is commonly grown in all continents of the world, largely in Asia and Europe [8]. *Coriandrum sativum* plant has been well documented for their generic usage in health functions, ayurvedic medicines and diversified biological activities [9].

Water stress significantly reduced the growth and development of *Coriandrum sativum* by distorting the morphogenesis, nutritional balance, biochemical and physiological activities. Further, under the influence of water stress, *Coriandrum sativum* plants produce reactive oxygen species (ROS) that oxidizes biomolecules, phytoconstituents and distort cellular functions. Therefore, *Coriandrum sativum* plants developed the strategy by adopting the mechanism of osmotic adjustment by the production of osmolytes, stimulation of antioxidant system and stomatal regulation by abscisic acid (ABA) production [10].

Currently, nanotechnology (nanoparticles; NPs) are becoming increasingly involved in agriculture as nanofertilizers due to cheapness in manufacturing together with the low consumption and low levels of phytotoxicity [11]. NPs possess novel properties due to its

small size and reactive nature. There are various kinds of NPs from metal-based to carbon-based. Taking into account all these NPs, Zinc oxide nanoparticles (ZnOx NPs) are the fourth largest utilized NPs in different sectors worldwide, especially in agriculture, where it acts as growth regulators and nanofertilizers [12]. The reason for their extensive use in agriculture due to its low energy band gaps, limited or non-availability of Zn in soil (causes adverse effects on crop) and its faster translocation rate within plant parts that improved the nutrient uptake [13–15]. Zinc is the main key factor for the proper functioning of metabolic machinery in plants and used it as micronutrient. It plays a vital role in the production of many enzymes, biosynthesis of chlorophyll and protein, cell division, maintenance of photosynthetic apparatus, and cell membrane stability [16]. Moreover, micronutrients such as Zn have been confirmed to relieve the plants from water stress by increasing water potential (Ψ_w), detoxifying the free radicals and ROS and maintaining the cell integrity [17]. In addition, foliar administration of NPs is more practical and easier to approach because plants may absorb them directly and a very low amount is required as compared to soil application [18]. We believe that the application of nanotechnology can assist to solve water scarcity issue.

Therefore, synthesis of metal-based NPs utilizing plant extract seems to be the best choice for large scale production. This is the most appealing method because of production of cost effective, defined size, biocompatible and ecofriendly stable NPs referred to as Green Synthesis [18]. Natural phytochemicals act as capping agents for the preparation of stable NPs [18]. A variety of plants have been reported for the green synthesis of ZnOx NPs such as *Moringa oleifera*, *Cassia fistula*, *Hibiscus subdariffa*, *Citrus aurantifolia*, *Aloe barbadensis*, *Laurus nobilis*, *Ocimum basilicum*, *Lippia adoensis* and *Lycopersicon esculentum* [19–26].

Studies reported that foliar applied ZnOx NPs improved the physiological process in *Zea mays* L., *Leucaena leucocephala*, *Pisum sativum* L. and *Beta vulgaris* L. by minimizing the malondialdehyde concentration and improved the antioxidative activities of enzymes and modulation of osmolytes under abiotic stress [27,28]. Numbers of studies are available that enlighten the role of ZnOx NPs in improving the tolerance under water stress in peanut, wheat, tomato, sorghum, maize, eggplant [29] and mung bean [17,30–34]. In above context, we believe that the application of nanotechnology can assist in solving the water scarcity issue.

Therefore, the current study was designed to provide a sophisticated and simple method for the green synthesis of ZnOx NPs with the following objectives. (a) To evaluate the efficacy of foliar applied ZnOx NPs against water stress regimes in *Coriandrum sativum* by profiling the antioxidant enzymes, chlorophyll and MDA content, and proline. (b) To determine the potential role of foliar applied ZnOx NPs in plant height, number of primary and secondary branches, number of umbels, umbellets per umbel, LAI, number of seeds and weight of 1000 seeds under water stress regimes. (c) To assess the efficient water stress regime for sustainable production of fresh biomass, dry biomass, EY and HI.

2. Material and Methods

2.1. Leaf Extract of Green Tea

The fresh green tea leaves were obtained from local market. These leaves were dried under shade for 7 days and grinded into refined powder form. It was stored in a glass jar for further use. Leaf extract was prepared by adding 100 mL of d.H₂O into 10 g of green tea dried leaves. The solution was heated and stirred continuously for 2 h by using a magnet stirrer. Then it was cooled down at room temperature. Filtered this cooled solution through Whatman filter paper No. 40. The filtrate was centrifuged at 4000 × g for 15 min to obtain the clear leaf extract.

2.2. Preparation of Zinc Oxide Nanoparticles (ZnOx NPs)

Nanoparticles were prepared by followed the method of [35] with some modifications. This was based on green synthesis from the green tea leaf. An amount of 0.2 M solution of Zinc acetate dihydrate [Zn(CH₃CO₂)₂·2H₂O] was prepared. Adding 230 mL of

$\text{Zn}(\text{CH}_3\text{CO}_2)_2 \cdot 2\text{H}_2\text{O}$ into 100 mL of leaf extract, a pale yellow color ZnOx NPs instantly formed. Then, this solution was placed in an incubator to attain dried brown crystals at 40 °C for 24 h. Calcination of these crystals were done at 100 °C for one hour. Cooled it at room temperature and stored in a glass bottle for further investigation and characterization.

2.3. Characterization of Zinc Oxide Nanoparticles (ZnOx NPs)

The quality of prepared ZnOx NPs were evaluated by performing the reported tests. The preliminary test was conducted for the initial confirmation of ZnOx NPs via UV spectroscopy. The optical spectroscopy was measured by using UV Spectrophotometer (Model) by dispersing the NPs into distilled water. The wavelength range were between 300 nm to 800 nm. The energy gap for ZnOx NPs ranges from 4.27–3.87 eV. Crystalline nature, morphology and structural properties were analyzed by X-ray diffractometer (XRD). The sample was exposed to a $\text{CuK}\alpha 1$ - for generating radiation with $\lambda = 1.5406 \text{ \AA}$. The scanning was done at 40 kV and 30 mA with 2θ ranging from 30°–140° to confirm the presence of ZnOx NPs. The phytochemical constituents and various functional groups that were involved in the reduction and stabilization of ZnOx NPs were identified through Fourier transform infrared spectroscopy (FTIR). It was carried out using the attenuated total reflectance (ATR) mode with a Jasco FTIR 4100 spectrophotometer (Japan). The results were obtained in the range of 400–4000 cm^{-1} . The surface morphology, composition of green synthesized NPs was characterized by scanning electron microscopy (SEM) equipped with energy dispersive X-ray spectroscopy (EDX) by using INSPECT F50 FEI, Netherlands.

2.4. Experimental Site, Design and Growth Conditions

The pot experiment was conducted at botanical garden of University of Education Lahore (Dera Ghazi Khan Campus), Punjab, Pakistan (129 m asl, 30°06' N and 70°62' E) in 2019/20. The average temperature from November to April was $25 \pm 3 \text{ }^\circ\text{C}$, respectively. The total annual precipitation was 173 mm. The physio-chemical analysis of soil is given in Table 1. Each pot contained 7.2 kg of soil and arranged in six vertical columns with respect to their treatments along with four replicates as shown in Figure 1. The presented study was designed to evaluate the response of plant to the foliar application of green synthesized ZnOx NPs under water stress conditions with reference to its agronomic characteristics. Therefore, a preliminary experiment was conducted before finalizing the experimental design and confirming the effective concentration of ZnOx NPs by applying different concentrations (50 ppm, 100 ppm, 200 ppm, 300 ppm) at 100% FC. The initial results confirmed that 100 ppm ZnOx NPs significantly regulates the plant growth and morphological features as reported in several studies [19,31,36]. Though, 100 ppm ZnOx NPs were used for foliar spray to explore its potential against water stress regimes.

Seeds sown in 2nd week of November. Weeds were manually controlled throughout the seasons. After the seedling establishment, plants were subjected to water stress based on maintenance of soil moisture at field capacity (SMFC). It was measured by saturating 7.2 Kg potted test soil without plants with water, and allowing the water to trench off completely for 12 h. Then, took 5 g of this soil for initial weight (Iw) in petri plate. Then dried this soil at 105 °C for 24 h and weighed it as final weight (Fw). Thereafter, calculate the SMFC % by given formula as Equation (1).

$$\text{SMFC \%} = (\text{Iw} - \text{Fw}/\text{Fw}) \times 100 \quad (1)$$

Table 1. Physiochemical analysis of soil.

Soil Texture	pH	EC (ms/cm)	FC (%)	BD (g/cm^{-3})	Cations (meq/100 g)			Anions (meq/100 g)			Saturation (%)	OM (%)	Particles Size Distribution (%)		
					K ⁺	Na ⁺	Ca ⁺⁺	Cl ⁻	CO ₃ ⁻²	HCO ⁻³			Sand	Silt	Clay
Clay Loamy	7.73	2.13	37.27	1.15	0.01	0.29	0.33	0.50	0	0.31	32	0.78	37.9	33.6	28.5

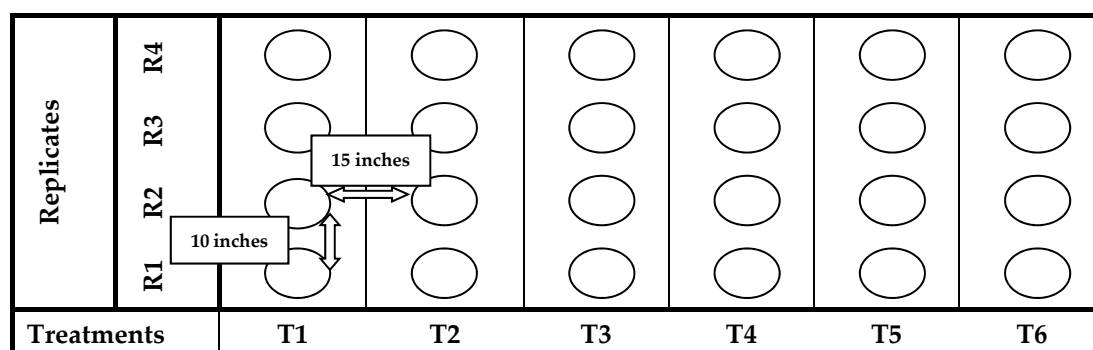


Figure 1. Design layout of pot experiment.

The point of reference for the next irrigation will be the 50% of SMFC of full irrigation (IR100). Therefore, on set of 50% SMFC in IR100, applying 75% and 50% irrigation to rest of plants corresponding to 50% SMFC of full irrigation to generate water stress regimes (IR50; intense level and IR75; moderate level). Therefore, inspection of depletion of water from field capacity was examined throughout the season by usual soil sampling on weekly basis through gravimetric method (105 °C, 24 h). Therefore, the following, six treatments were designed: T1 = IR100, T2 = IR100 + ZnOx NPs, T3 = IR75, T4 = IR75 + ZnOx NPs, T5 = IR50, T6 = IR50 + ZnOx NPs with four replicates.

Five plants were maintained in each pot by thinning. Water stress was applied after 15 days of seedling establishment. After 10th day of applying water stress foliar application of 100 ppm ZnOx NPs (2 mL per pot) initiated and continued for three times at regular interval of 10 days.

2.5. Enzymes Assay

One gram of plant leaf tissue was homogenized in 1 mL of 0.1 M sodium phosphate buffer (pH 6) at 4 °C and centrifuged. The homogenate was centrifuged at 12,000× *g* for 15 min at 4 °C and the supernatants were stored at −80 °C until used for the assay of peroxidase (POD) and catalase (CAT) activities. The peroxidase (POD) activity was evaluated by following the [36] protocol using guaiacol as substrate and considering that an increase in absorbance at 470 nm min^{−1} equals to POD activity (Liang et al., 2011). The catalase (CAT) activity was assayed by calculating the decrease in H₂O₂ at an optical density of 240 nm considering one unit activity equivalents to CAT quantity that breaks down 1 μmol of H₂O₂ in one minute [37,38]. The activity of Superoxide Dismutase (SOD) enzyme is assayed as described by [39,40] and calculated as [41]. The activity is indicated as number of units. One unit is defined as the amount of SOD that inhibits 50% of NADH oxidation. Method of [42] was used to measure the activity of APX due to ascorbate oxidation based on H₂O₂. This decomposition of ascorbate determined the decrease in absorbance at 290 nm. One milliliter of mixture (Potassium phosphate = 50 mM, ascorbate = 0.5 mM, EDTA = 0.1 mM) reacted with H₂O₂ (0.1 mM) for oxidation of ascorbate. APX activity was evaluated on the as the quantity of enzymes responsible for the production of oxidized ascorbate at the rate of 1 μmol/min.

2.6. Estimation of Chlorophyll and Proline

Chlorophyll a, b and total chlorophyll content (mg/g) were calculated using the method of [43,44]. Proline content (μM/g.f.wt.) estimation was carried out using the method described by [45].

2.7. Determination of Lipid Peroxidation (Malondialdehyde (C₃H₄O₂))

Malondialdehyde (MDA) was calculated using 2-thiobarbituric acid (TBA) as described by [46]. Taken a 1 g fresh leaf of *Coriandrum sativum* L. and ground with 5 mL 0.6% prepared TBA in 10% TCA (trichloroacetic acid; C₂HCl₃O₂), using a mortar and pestle.

This mixture was heated for 15 min in an oven for at 100 °C. Cooled down mixture in a thermos containing ice and centrifuged at $5000 \times g$ for 12 min. The absorbance of the supernatant has been recorded at 450 to 600 nm. The contents of MDA were determined according to a fresh weight as follows by Equation (2) [47]:

$$\text{MDA } (\mu\text{mol g}^{-1} \text{ FW}) = 6.45(\text{OD}_{532} - \text{OD}_{600}) - 0.56(\text{OD}_{450}) \quad (2)$$

2.8. Measurement of Agronomic Parameters

Harvested plants were moved to laboratory after 90 days of seedling establishment and certain features were measured per plant including plant height, number of primary and secondary branches, number of umbels and umbellets per plant and leaf area index of plants. Leaf Area was measured through the gravimetric method [48]. After drying the plants at $70 \pm \text{C}$ for 72 h in the oven, a dry weight was determined. Leaf area index was measured through the given formula:

$$\text{Leaf area index} = \text{Leaf area (mm}^2\text{)}/\text{Land cover (mm}^2\text{)} \quad (3)$$

The Leaf Area Index (LAI) is the entire surface area of the leaf per unit area of the land.

The yield attributes were estimated as fresh biomass, dried biomass, number of seeds, weight of 1000 seeds, economic yield (EY = seed yield) and harvest index [48]. The formula of HI is given below [49]

$$\text{HI} = \text{EY}/\text{Dry biomass} \times 100 \quad (4)$$

3. Results

The green synthesis based on the plant accumulates that contains metal ions and active phytochemicals. These constituents act as reductant agents and stabilizers. The Zinc acetate dihydrate reduced into ZnOx NPs, notified by a change in color of the reaction mixture. Clear demonstration of color change in reaction mixture caused by ZnOx NPs formation was given in Figure 1a.

3.1. UV-Vis Spectroscopy

Green synthesized NPs of ZnOx was analyzed optically through UV spectroscopy. The given UV spectra showed a sharp absorption band at 376 nm (Figure 2b). This band confirmed the presence of ZnOx NPs. Though, there was no other absorption peak in the spectra that showed that the product being produced is pure ZnOx NPs. This absorption intensity was obtained when the calcination of sample NPs done at 100 °C.

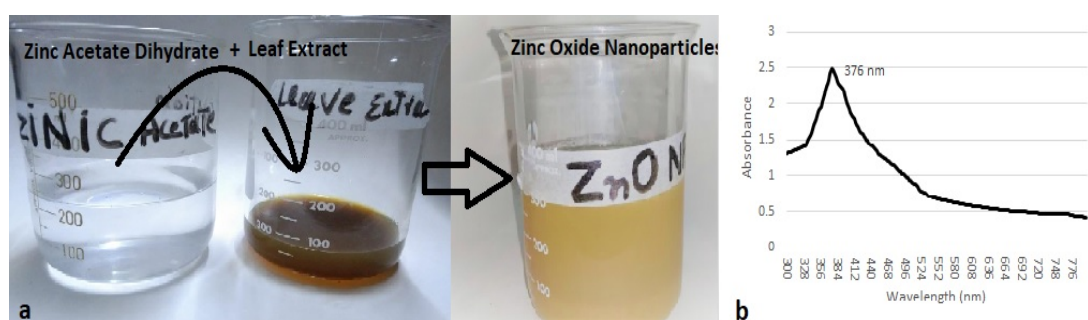


Figure 2. Optical characteristics. (a) Reduction of Zinc acetate dihydrate into green synthesized ZnOx NPs confirmed by change in color of reaction mixture. (b) Confirmation of ZnOx NPs through absorption peak of UV-visible spectroscopy.

3.2. X ray Diffraction (XRD)

XRD graph of ZnOx NPs was shown in a Figure 3a. It showed distinct peaks against 2 Theta in micrograph at 31.82°, 34.45°, 36.23°, 47.50°, 56.51°, 62.82° and 67.93° corresponds to (100), (002), (101), (102), (110), (103) and (200), respectively, lattice planes confirmed the nanoscale range of prepared ZnOx NPs. All these peaks were indexed by using JCPDS card No. 036-1451 that confirmed the crystalline morphology of ZnOx NPs from non-smooth partial spherical to hexagonal wurtzite. The crystalline size (D) of prepared NPs was measured by using the Debye Scherrer formulae based on wavelength Cu Ka 1.5406 °Å, Bragg's diffraction angle (θ) and full width at half-maximum (β) of most intense peak (101) corresponding to 2 θ

$$D = (0.9 \times \lambda) / (\beta \times \cos\theta) \quad (5)$$

3.3. Fourier Transform Infrared Spectroscopy (FTIR) and Particle Size Distribution

FTIR showed distinct peaks of different functional groups in the prepared samples of NPs as shown in Figure 3b. A wide stretch is present between 3000 to 3400 cm^{-1} with maximum absorption at 3091 cm^{-1} in a region of high energy due to stretching of $-\text{NH}_2$ - and $-\text{OH}$ group of alcohol and phenol. The absorption peak at 2359 cm^{-1} specifies the presence of CO_2 molecules. The sharp band peak at 1547 cm^{-1} shows the stretching of C-C of aromatic rings. The prominent absorption intensity at 1427 is due to the frequencies of stretching of C-N of amide I and $-\text{CH}_2$ (vibrations of scissoring proteins) or bending vibration of $\alpha\text{-CH}_2$ of ketones and aldehydes. Two weak peaks at 1016 and 941 is due to vibrational stretch frequencies of C-O of amino acid and alcohol; C-N stretch of amine. The peak that ranges from 500 to 683 cm^{-1} designates the stretching vibration of hexagonal ZnOx NPs. The average particle size was 37 nm as shown in Figure 3c. The maximum number of particles were present between a range of 20 nm to 40 nm indicated a normal distribution.

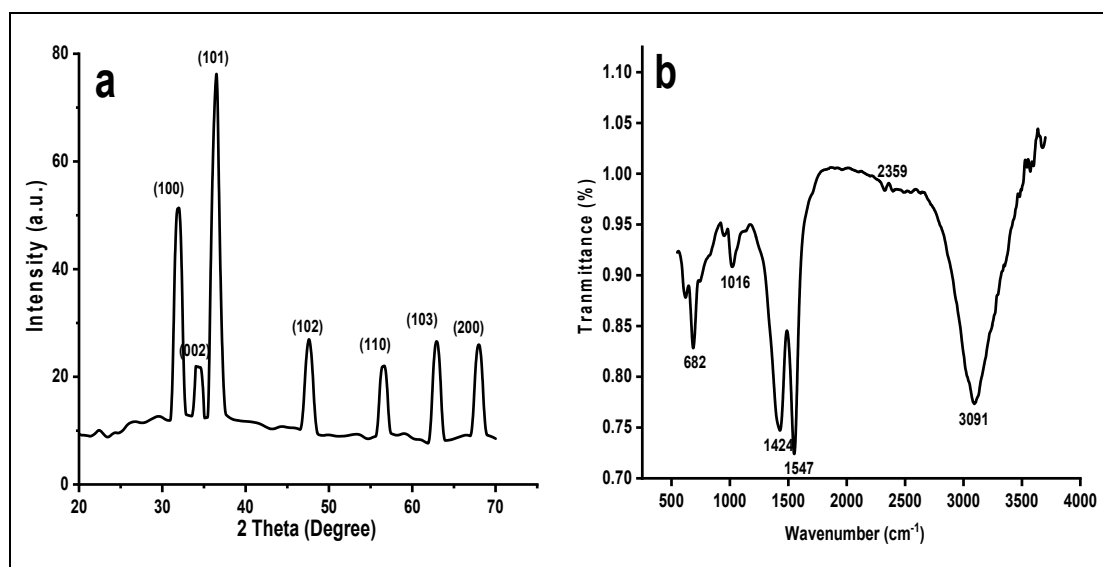


Figure 3. Cont.

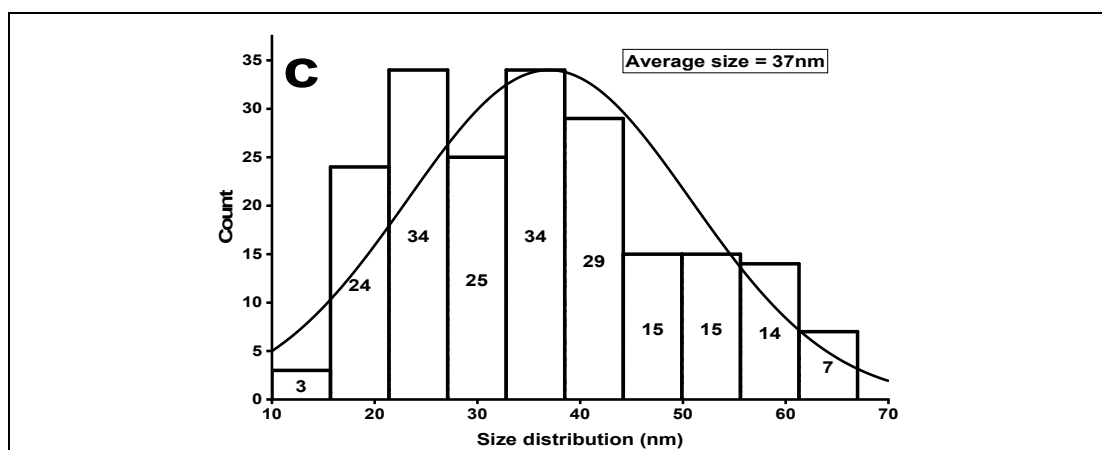


Figure 3. (a) XRD of green synthesized ZnOx NPs. (b) FTIR of green synthesized ZnOx NPs. (c) Size distribution of ZnOx NPs.

3.4. Scanning Electron Microscopy (SEM)

The surface morphology of green synthesized ZnOx NPs thoroughly studied through SEM. The micrographs of SEM are shown in Figure 4a–d that revealed the nano size range. The surface image of the particles showed non smooth semispherical to hexagonal wurtzite shape and few are non-spherical monoclinic particles having agglomerated form. The morphological structure and size of particle were observed by using the SEM micrographs using Image J software. The green synthesized ZnOx NPs was confirmed by comparing the particle size from XRD and SEM produced image.

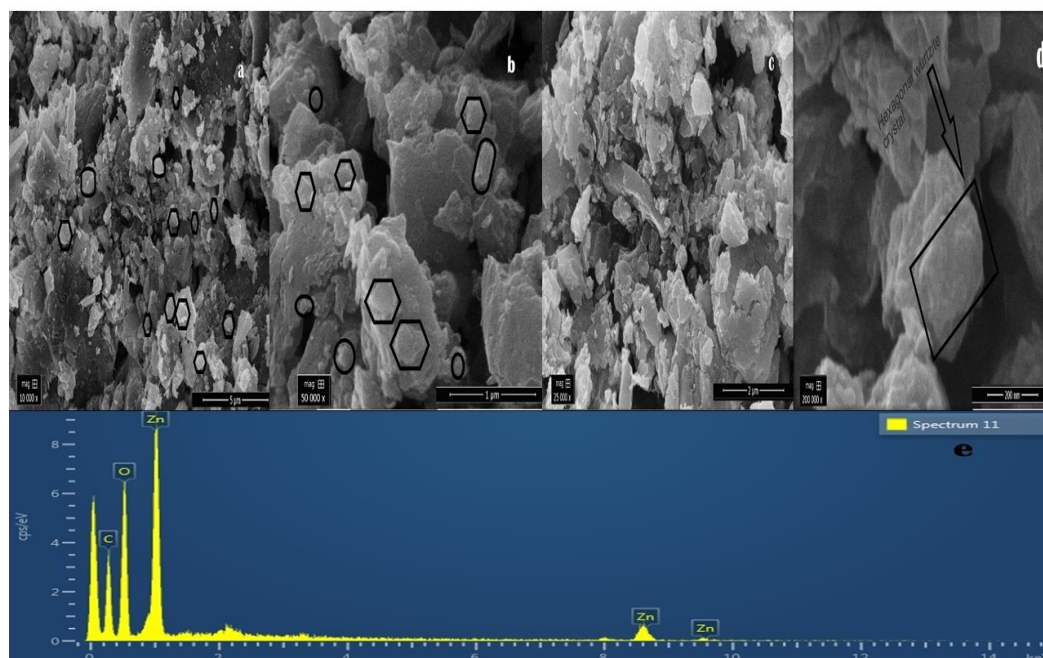


Figure 4. SEM (Scanning electron microscopy) of green synthesized ZnOx NPs at different magnification. (a) 10,000× at 5 μm scale. (b) 50,000× at 25,000 μm scale. (c) 50,000× at 1 μm scale. (d) 200,000× at 200 nm scale. (e) EDS (Elemental dispersive spectroscopy) spectrum of green synthesized ZnOx NPs indicating weight % of elements.

3.5. Elemental Dispersive Spectroscopy (EDS)

Elemental analysis of prepared nanoparticles was performed through EDS technique shown in Figure 4e. This analysis showed the stoichiometric ratio of Zn and O along with other elements. EDS spectra confirmed that presence of ZnOx NPs. EDS analysis showed

in three peaks between 1 to 10 kV that are associated with zinc present in prepared sample. Further, it mentioned the weight percentage of Zn (52.22), O (34.40%) and C (13.38%) and the purity of NPs.

3.6. Effect of Green Synthesized ZnOx NPs on the Activity of Some Antioxidant Enzymes

Under water stress, plant is enabled to produce antioxidant enzymes. Mainly, it possesses peroxidases, catalases and superoxide dismutase. Results in Figure 5A–D presented that the activity of POD, CAT, APX and SOD that increased in IR75 (32%, 78%, 81% and 10%) and IR50 (40%, 163%, 209% and 63%) with respect to full irrigated plants. Whereas POD activity is reduced in all irrigation levels including stress regimes with maximum reduction found in full irrigated plants treated with ZnOx NPs, the foliar application of green synthesized ZnOx NPs escalated the activity of CAT, APX and SOD two-fold in water stress regimes.

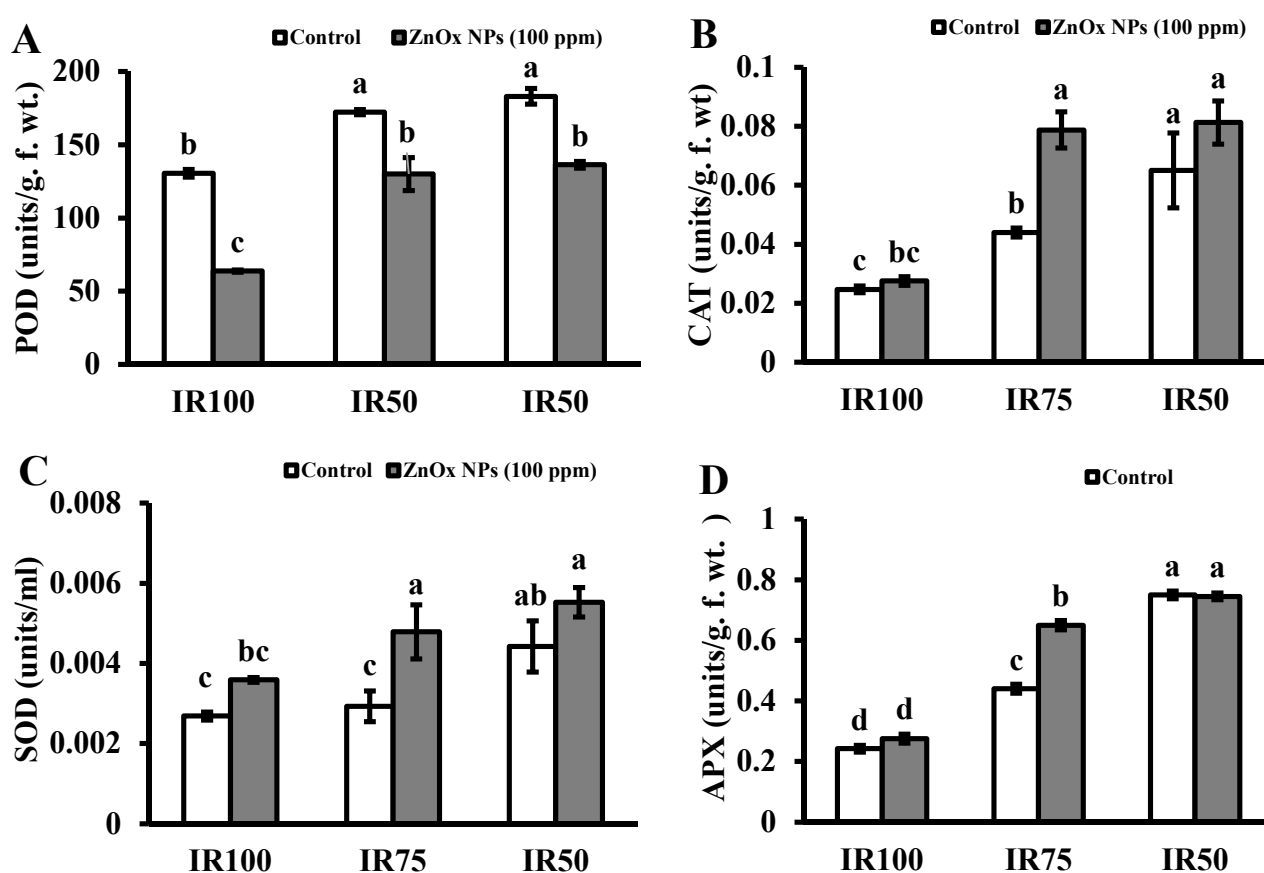


Figure 5. Effect of ZnOx NPs on antioxidant enzymes. (A) Peroxidase activity under full irrigation IR100 and water stress regimes IR75 and IR50. (B) Catalase activity under full irrigation IR100 and water stress regimes IR75 and IR50. (C) Sodium dismutase activity under full irrigation IR100 and water stress regimes IR75 and IR50. (D) Ascorbate peroxidase activity under full irrigation IR100 and water stress regimes IR75 and IR50. Data presented in bars is mean value of 4 replicates \pm SE of treatments bearing same letters were not significantly different at $p \leq 0.05$ by LSD.

3.7. Effect of Green Synthesized ZnOx NPs on Chlorophyll Content

The growth of plant greatly reduced under water stress due to decreased in chlorophyll content as shown in Figure 6A,B. The chlorophyll a and b both decreased as water stress increased from 3% to 7% and 14% to 34% at IR75 and IR50. Plants treated with ZnOx NPs significantly increased the chlorophyll pigment with maximum value found in IR50 of chlorophyll b that was 33.5 mg/g. f. wt. compared to non-treated ZnOx NPs plants.

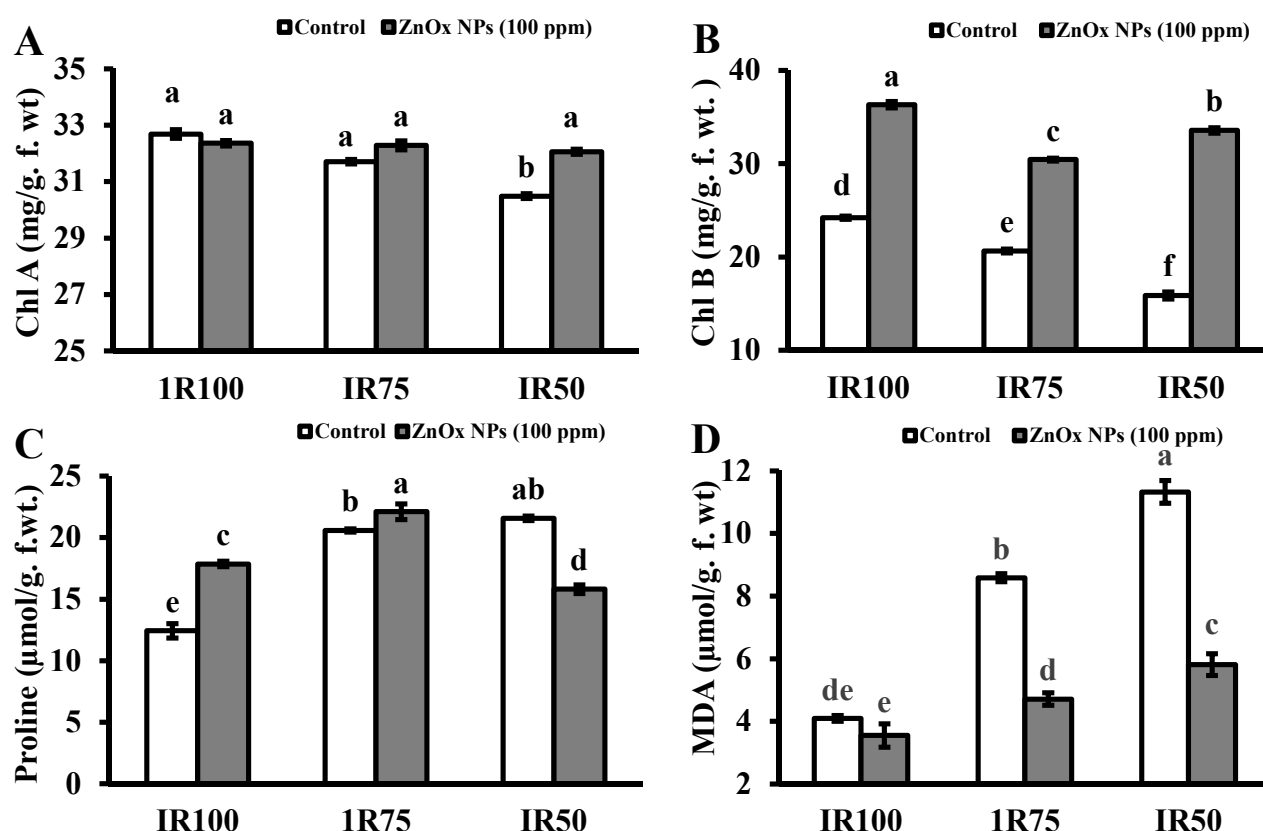


Figure 6. Effect of ZnOx NPs on: (A) Content of chlorophyll a under full irrigation IR100 and water stress regimes IR75 and IR50. (B) Content of chlorophyll b under full irrigation IR100 and water stress regimes IR75 and IR50. (C) Amount of proline under full irrigation IR100 and water stress regimes IR75 and IR50. (D) Malondialdehyde content under full irrigation IR100 and water stress regimes IR75 and IR50. Data presented in bars is mean value of 4 replicates \pm SE of treatments bearing same letters were not significantly different at $p \leq 0.05$ by LSD.

3.8. Effect of Green Synthesized ZnOx NPs on Proline and Lipid Peroxidation (MDA)

The proline concentration was significantly increased under water stress in *Coriandrum sativum*. Figure 6C revealed the increased of proline content 75% to 83% under water stress regime IR75 and IR50. Although the foliar application of ZnOx NPs further enhanced the proline concentration with maximum 22% in IR75 while it reduced in IR50 to 11% with respect to non-treated ZnOx NPs plants. MDA content significantly increased one and two-fold in water stress regime IR75 and IR50 compared to non-treated ZnOx NPs plants as shown in Figure 6D. On the other end the ZnOx NPs has lower the MDA content in full irrigation and water stress regimes.

3.9. Effect of Green Synthesized ZnOx NPs on Agronomic Attributes

All the investigated agronomic attributes significantly reduced under water stress irrigation in *Coriandrum sativum*. It includes vegetative as well as yield parameters. Foliar applied ZnOx NPs significantly improved the observed agronomic parameters by enabling the plants to become tolerant against water stress.

3.9.1. Plant Height

The maximum plant height (51 cm) was observed in full irrigation. Water stress greatly reduced the plant height of *Coriandrum sativum* in IR75 (45%) and IR50 (51%) compared to IR100. Additionally, the foliar application of 100 ppm of ZnOx NPs significantly increased the plant height by 8% in full irrigation (IR100) as well as 15% and 40% in water stress regimes IR75 and IR50 compared to non-treated ZnOx NPs plants as shown in Figure 7A. The maximum significant effect was observed in IR50.

3.9.2. Numbers of Primary and Secondary Branches

Statistical analysis revealed that primary branches are not significantly affected by the water stress regimes (Figure 7B). The secondary branches significantly reduced to 5% under both moderate and intense water stress regimes (IR75 and IR50) compared to full irrigation plants as shown by Figure 7C. Similarly, the application of 100 ppm of ZnOx NPs has no significant effect on numbers of primary branches, while it significantly increases the numbers of secondary branches in all irrigation regimes. The maximum increase of two-fold was observed in IR75 followed by one and half fold increase in IR50 under water stress conditions. Nevertheless, only a 29% increase was observed in IR100 due to foliar applied ZnOx NPs.

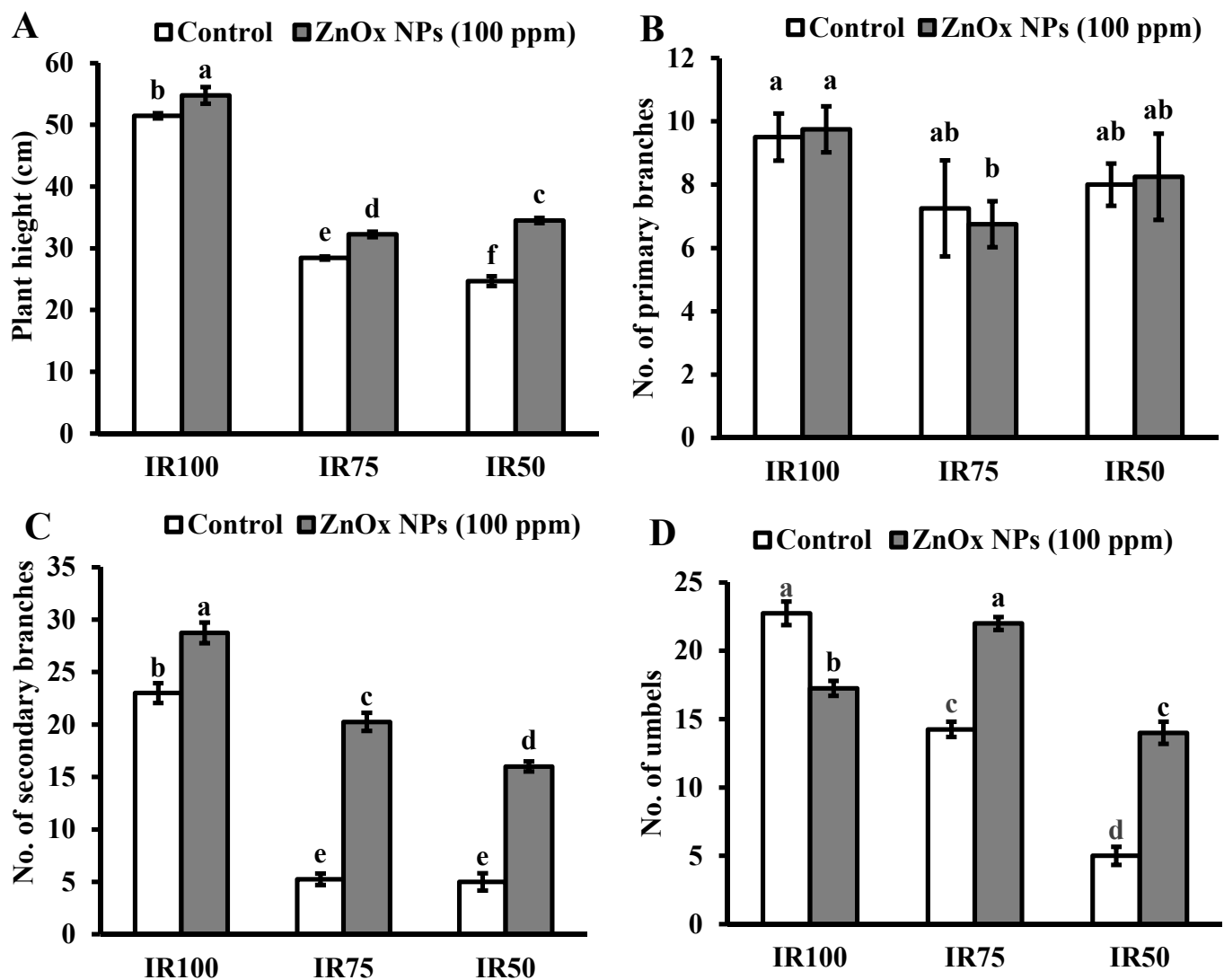


Figure 7. Cont.

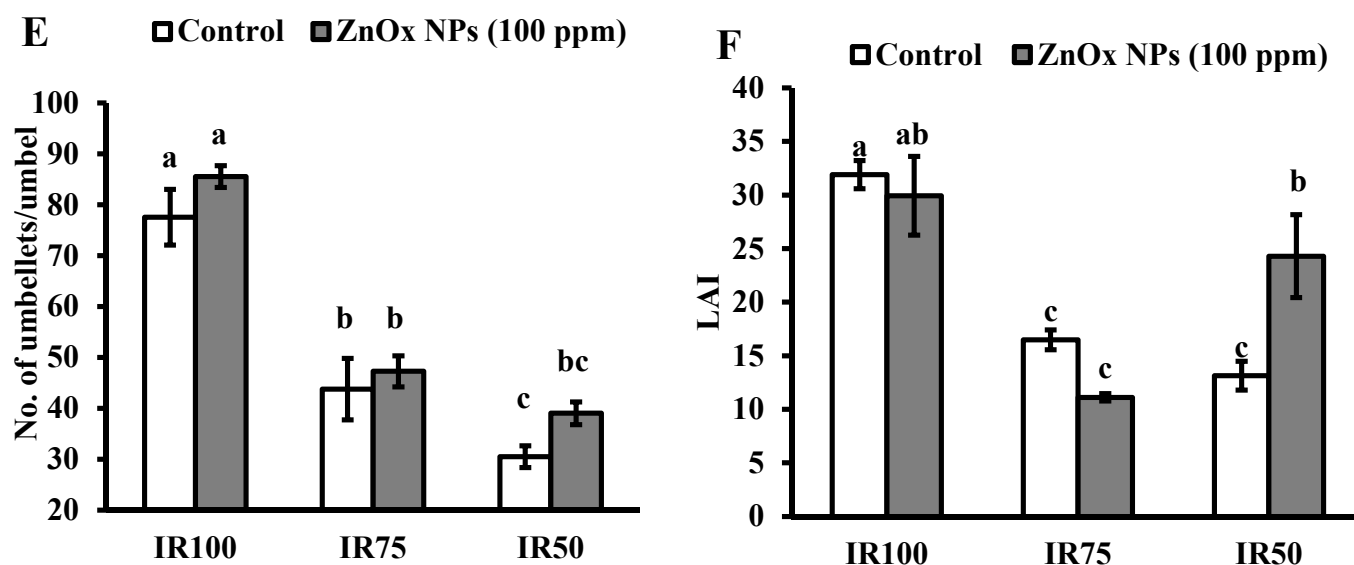


Figure 7. Effect of ZnOx NPs on: (A) Plant height under full irrigation IR100 and water stress regimes IR75 and IR50. (B) Number of primary branches per plant under full irrigation IR100 and water stress regimes IR75 and IR50. (C) Number of secondary branches per plant under full irrigation IR100 and water stress regimes IR75 and IR50. (D) Number of umbels per plant under full irrigation IR100 and water stress regimes IR75 and IR50. (E) Number of umbellets per umbel under full irrigation IR100 and water stress regimes IR75 and IR50. (F) LAI (leaf area index) per plant under full irrigation IR100 and water stress regimes in IR75 and IR50. Data presented in bars is mean value of 4 replicates \pm SE of treatments bearing same letters were not significantly different at $p \leq 0.05$ by LSD.

3.9.3. Number of Umbels and Umbellets Per Umbels

Water stress regimes significantly reduced the number of umbels per plant. The reduction was 40% in IR75 and more than two-fold in IR50 compared to IR100 (Figure 7D). Though, umbellets per umbel were also reduced on the account of moderate and intense water stress regimes. Results showed 44% decrease in IR75 and 61% in IR50 in number of umbellets per umbel with respect to IR100 plants. However, the foliar application of ZnOx NPs (100 ppm) efficiently increase the numbers of umbels (58% and 7%) and umbellets per umbel (almost one and half fold and 26%) in IR75 and IR50 compared to non-treated ZnOx NPs plants (Figure 6D,E).

3.9.4. Leaf Area Index (LAI)

Likewise, water stress significantly effects LAI of *Coriandrum sativum* plants in IR75 and IR50 while the main effect of treatments T2 and T4 showed non-significant results in IR100 and IR75. Under water stress regimes, the LAI was decreased to 50% in IR75 and 60% in IR50 (Figure 7F) compared to full irrigation plants. Application of 100 ppm ZnOx NPs showed significant result in IR50 plants that increase the LAI to 85%, while it reduced the LAI in IR100 (7%) and IR75 (32%) compared to untreated ZnOx NPs plants.

3.9.5. Fresh and Dry Biomass

Plant fresh and dry biomass were significantly decreased under water stress regimes compared to full irrigated plants. Decreases in fresh biomass of plants were observed, 59% and 80%, while dry biomass was 67% and 84% in IR75 and IR50 compared to IR100 plants. In addition, T4 (IR75) and T6 (IR50) treatments showed non-significant results under water stress irrigation in case of fresh biomass, while the maximum increase of 33% was found in IR100 treated with 100 ppm of foliar applied ZnOx NPs. (Figure 8A). Similarly, IR50 showed non-significant effects in plant dry biomass. Significant increase of 34% and 50% in plant biomass was observed in IR100 and IR75 compared to non-treated ZnOx NPs plants (Figure 8B).

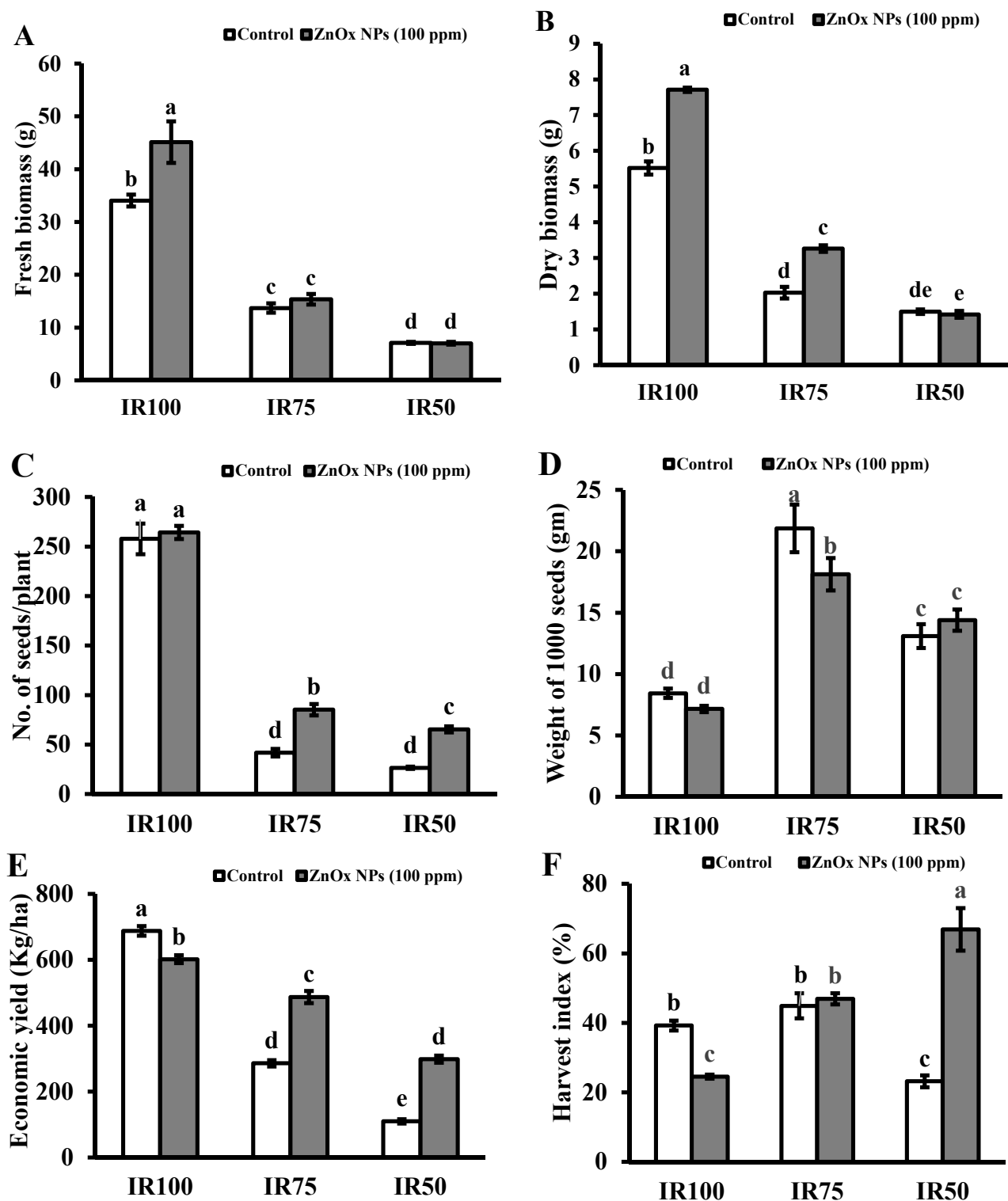


Figure 8. Effect of ZnOx NPs on: (A) Fresh biomass per plant under full irrigation IR100 and water stress regimes IR75 and IR50. (B) Dry biomass per plant under full irrigation IR100 and water stress regimes IR75 and IR50. (C) Number of seeds per plant under full irrigation IR100 and water stress regimes IR75 and IR50. (D) Weight of 1000 seeds under full irrigation IR100 and water stress regimes IR75 and IR50. (E) Economic yield under full irrigation IR100 and water stress regimes IR75 and IR50. (F) Harvest index (HI) under full irrigation IR100 and water stress regimes in IR75 and IR50. Data presented in bars is mean value of 4 replicates \pm SE of treatments bearing same letters were not significantly different at $p \leq 0.05$ by LSD.

3.9.6. Number of Seeds and Weight of 1000 Seeds

Statistical analysis showed that the number of seeds greatly reduced to 84% and 94% in IR75 and IR50 plants compared to IR100 plants (Figure 8C). Contrary to this, the weight of 1000 seeds were significantly increased under water stress regimes to almost one and half fold (175%) in IR75 and 63% in IR50 compared to fully irrigated plants (Figure 8D). Correspondingly, IR75 and IR50 plants showed significant increase in number of seeds to one-fold and more than one-fold under water stress regimes compared to non-treated ZnOx NPs in IR75 and IR50 plants. While the weight of 1000 seeds in IR100 and IR50 treated with foliar applied ZnOx NPs showed non-significant results contrast to their non-treated ZnOx NPs plants, the maximum reduction of 19% was observed in T4 plants compared to T3 plants. The weight of 1000 seeds increased to 8% in IR50 after the foliar application of ZnOx NPs (100 ppm).

3.9.7. Economic Yield

Significant decrease in economic yield was found under water stress regimes IR75 and IR50 with respect to full irrigation IR100. The decrease was 59% in T3 and 84% in T5 compared to T1 plants. Foliar application of ZnOx NPs (100 ppm) significantly increase the economic yield in *Coriandrum sativum* under water stress in IR75 and IR50 (Figure 8E). The treatment T4 (IR75) and T6 (IR50) showed 71% and more than one-fold increase in economic yield compared to non-treated ZnOx NPs plants.

3.9.8. Harvest Index

Results revealed that water deficit irrigation decreases the HI to 41% in IR50 while a non-significant effect was shown by IR75 under water stress regimes in contrast to full irrigated T1 plants (Figure 8F). ZnOx NPs significantly increased HI to almost one and half fold in IR50 in comparison to non-treated ZnOx NPs plants. Additionally, application of ZnOx NPs decreased the HI to 36% in IR100 (T2).

4. Discussion

The most convenient and efficient method was used in the green synthesis of ZnOx NPs by using leaf extract of *Camellia sinensis* L., and zinc acetate dihydrate was used as precursor. The formation of ZnOx NPs was confirmed by changing in color of the reaction mixture. It could be due to the excitation of surface vibration of NPs that results into Surface Plasmon Resonance as reported by many studies [50,51]. Further, it may be attributed by the presence of flavonoids and phenols in the leaf extract that held responsible for the biosynthesis of ZnOx NPs from Zn ions. Clear demonstration of color change in reaction mixture caused by ZnOx NPs formation was given in Figure 1a. These findings of color changes were in line with the earlier reported studies in green synthesized ZnOx NPs production [52,53].

However, reports revealed that ZnOx NPs have a typical wide absorption spectrum range between 330–460 nm [54,55]. The results are in agreement with the findings of Bala et al. [22]. It was found that the calculated band gap was at 3.37 eV. This band gap of ZnOx NPs could be due to the transmission of e^- from valence band to the conducting bands as described by Xaba et al. [56]. Furthermore, the literature stated that intensity of peak in UV vis spectra is associated with NPs size and blue shifted absorption that based on reduction in crystal size [57]. Consequently, the energy gap increased by decreasing the NPs size. So, an inverse relationship between band gap and wavelength of absorption peak was observed as described by [21]. This blue shift is just because of quantum confinement effect of individual nanoparticles as described in literature [55]. These results conformed the standard ZnOx absorption spectra, as all metallic oxides exhibit broad band gaps with shorter wavelengths. Our results for green synthesized ZnOx NPs support this idea here.

In this regard, it has been found that all the typical peaks that were associated with ZnOx NPs are in consistent with the findings of earlier reported studies [24,58,59]. The average crystalline size is 37 nm, which is very close to the results of existing reports [60,61].

Further, the functional group showed by FTIR results are in harmony with the findings of earlier literature [62]. The presence of CO₂ in band peak at 2359 cm⁻¹ showed as residual substance. The spectra of FTIR revealed that the molecules of proteins and phytoconstituents found in the leaf extract of *Camellia sinensis* causes the reduction of metal ions as described by previous studies [63]. Moreover, the peaks present within the range of 400 to 680 assured the presence of hexagonal wurtzite ZnOx NPs due to phyto-accumulates of plants that provide the stability [64]. These findings are in coherence with the study of [50,57] that further supported the formation of required NPs using the phytochemicals as a capping and reducing agent of leaf extract. These results suggested that the hydroxyl group of alcohol, flavonoids, phenols, molecules of protein and various other functional group play a key role in the formation of stabilized ZnOx NPs.

The surface morphology of ZnOx NPs is in harmony with NPs of [20]. Further, this agglomeration within ZnOx NPs could be the result of electrostatic attraction of ZnOx NPs and polarity as described by [61]. The green synthesized ZnOx NPs was further confirmed by comparing the particle size from XRD and SEM produced image. These results are in harmony of available reports [65–68].

Previous reports have shown evidence that the stimulation of antioxidant system of plants occurs by producing antioxidative enzymes under water stress to prevent cellular damage [69]. These findings follow the trend of Hu et al. [70] in *Salvinia natans* L. that reduced the POD activity and enhanced the CAT and SOD activity after the application of 25 nm ZnOx NPs. Similar results have been found in another study conducted in *Gossypium hirsutum* L. [71]. A study by Sharifi-Rad et al. [72] described the application 100 ppm of the ZnOx NPs to *Momordica charantia* L. that significantly boosted the activity of CAT, endorsing the validity of our findings. Plants with higher activities of these enzymes showed high ROS scavenging ability, which reflects the water stress tolerant nature in the plant. The impact of water stress in antioxidant activity is multifaceted and rely on the extremity of water stress and plant variety.

The increase in concentration of Chl a and Chl b on the account of foliar application of ZnOx NPs under water stress are in accordance to findings of Gurmani et al. [73] who described the role of Zn in enhancement of chlorophyll content in tomato. The same approach has been observed in another study in *Lupinus termis* [74]. The reason behind this increase could be the role of ZnOx in carbonic anhydrase (Zn metalloenzymes). This is a Zn derivative enzyme that facilitates efficient utilization of carbon dioxide in plants. A number of studies have been reported that showed alternative results on the account of ZnOx application [75]. This may be the attribute of species-to-species adaptation and variation in response of ZnOx utilization. Higher concentration of ZnOx also affect the physiochemical activities of plants. Therefore, more research is required to evaluate the behavior of different plants on the exposure of green synthesized Zn based nanoparticles.

The decrease of MDA is associated with the increase in CAT and SOD activity as described by Ahmad et al. [76]. Reactive oxygen species were produced as a result of water stress that oxidized the lipid component of membrane mediated by the production of MDA [77]. The osmolytes such as proline also play an important role in detoxifying the ROS, forming the complex substance with them and ultimately restricting the lipid peroxidation. Therefore, it could be associated with water stress tolerance in plants. Further, under water stress conditions, the plants adopted a strategy of osmotic adjustment for the functioning of physiological machinery by the production of these compatible cellular solutes [78].

Plant height was decreased under water stress regimes, indicated by the stunted growth in *Corinandrum sativum*, compared to full irrigation as shown by result of current study, it may be attributed to the decrease in turgidity of cell, loss of turgor pressure and dehydration of cytosol, which in turn resulted into reduction of cell division and enlargement. The current finding is consistent with Tiwari et al. [79]. The reduction of plant height was also reported by Mushtaq et al. and Memon et al. [80,81].

Coriandrum sativum adopt a unique approach by reducing the secondary branches and LAI as response against water stress regimes due to loss of turgor pressure that reduced the rate of transpiration and affects the metabolic machinery and cell expansion in *Coriander sativum* plants [82]. Similarly, the number of umbels and umbellets per umbel were also reduced in water stress regimes compared to full irrigation. Water stress regimes can decrease the leaf water potential, as a result of which the relative water content decreases which can inhibit the cell division and differentiation and reduce the number of umbels and umbellets per umbel in *Coriander sativum*. These results are consistent with earlier reported studies [83,84]. This could be an escaping mechanism to prevent the water loss by reducing the vegetative growth and LAI as a result the evapotranspiration decreases from the leaf surface that affected the photosynthetic machinery, meristem activities, cell differentiation and overall growth of plants [85].

Plant fresh and dry biomass were severely reduced in IR75 and IR50. Several reports have documented the reduction in fresh and dry biomass during water deficit stress. This could be an indicator for describing the susceptibility of *Coriandrum sativum* plants to tissue and cell desiccation [86,87].

Number of seeds greatly reduced under water stress regimes. Number of seeds showed a contrary response to weight of 1000 seeds under water stress regimes in *C. sativum*. Presented results showed that under water stress, irrigation plants that exhibit greater number of seeds were low in weight, which reduced the weight of 1000 seeds per plant and vice versa. It can be assumed that the number of seeds have contradictory relationship to the weight of 1000 seeds [88]. Similarly, an opposite link between seed weight and number of seeds/plants also shown by a study on oilseed rape [89]. It could be due the source–sink relationship that is involved in the distribution of photosynthates in seeds on account of water stress. It may be attributed to limitation in translocation of photo-assimilates for seed filling from source (leaves) under water shortage that may cause reduction in weight of seeds [90].

The EY of *Coriandrum sativum* significantly reduced under water stress regimes. The reduction of EY could be the result of variation in various mechanisms. It includes delayed anthesis, reduction in leaf area, decrease in chlorophyll content and photosynthetic activity, abnormal expression of water stress response genes, distorted distribution of photoassimilates during seed filling that resulted into overall decrease in EY of *Coriandrum sativum* under water stress regimes IR75 and IR50 [91]. Our result is in agreement with previous reported studies [92–94]. Presented results revealed that HI were significantly reduced in severe water stress regimes (IR50).

Plants that were treated with ZnOx NPs showed increase in plant height and number of secondary branches under water stress regimes. It could be due to the involvement of Zn in synthesis and regulation of various enzymes that enhanced the cell division and expansion as described by Dimkpa et al. [17].

ZnOx NPs increase the relative water content *Coriandrum sativum* that can help to maintained the cell membrane stability and promote mitotic activity under water stress to increase the number of umbels and umbellets per umbel and LAI as reported in previous studies [95]. Presented results revealed that NPs significantly increase the fresh and dry biomass of *Coriandrum sativum* in full and moderate irrigation regime (IR100 and IR75). Similarly, Dhoke et al. [96] found that application of ZnOx NPs increase the fresh and dry biomass in *Vigna radiata* plants under water deficit stress. The increase in number of seeds after being treated with NPs in the current study can be due to improved translocation of N and K, which are involved in the formation of seeds. This finding is in harmony with a previous study [17]. Further literature stated that these NPs increased the chlorophyll content, stomatal conductance, leaf water potential, transpiration rate and water use efficiency under drought conditions that improved the photosynthesis and economic yield [11,97]. This might be the result of accumulation of secondary metabolites and osmolytes (osmo-protectant) for osmotic adjustment under water shortage conditions that improve the photosynthesis as well as overall yield of *Coriandrum sativum* and increase

the HI of the crop [98]. In the end, we assumed that ZnOx NPs increased the tolerance of *Coriandrum sativum* against water stress by enhancing the antioxidant enzymes activity, decreasing the ROS and improving the plant biomass to provide sustainable plant growth and economic yield.

5. Conclusions

In this study, NPs of ZnOx were synthesized by using the leaf extract of *Camellia sennesis* using precursor (Zinc acetate dihydrate). UV spectrum provided a peak at 376 nm that exists within the range of green ZnOx NPs. The efficiency of crystalline feature and synthesis method were further confirmed by XRD peaks. The average size of ZnOx NPs was confirmed by the analysis of XRD and SEM was found to be 37 nm. Functional group of phytoconstituents that act as capping and stabilizing agents were identified through FTIR analysis that endorsed the formation of ZnOx NPs. Foliar application of 100 ppm green synthesized ZnOx NPs improved the defensive mechanism of *Coriander sativum* L. under two regimes of water stress. ROS produced as the result of water stress. These NPs enhanced the activity of antioxidant enzyme CAT, SOD and APX along with chlorophyll content under the influence of water stress. ROS was produced as a result of water stress and MDA content decreasing as production of proline and enzymes activity increased. The maximum activity of antioxidant enzymes and MDA content was observed in IR50 while the amount of proline was higher in IR75. The agronomic attributes such as plant height, number of secondary branches, number of umbels and umbellets per umbel, fresh biomass, dry biomass, number of seeds, EY and HI were significantly increased due to foliar application of ZnOx NPs under water stress regimes. The number of primary branches and LAI showed non-significant results under water stress conditions. Moreover, the weight of 1000 seeds decreased in full (IR100) and moderate irrigation (IR75), while increasing in severe water stress regime (IR50). The maximum results of agronomic attributes were found in IR75, except the LAI and HI that were at maximum in IR50. Overall, the water stress regime IR75 showed efficient results on the account of foliar applied of 100 ppm of ZnOx NPs. Our study assured the simplest approach for the synthesis of ZnOx NPs through green synthesis and exposed the potential of 100 ppm of ZnOx NPs in alleviation of drought tolerance in *Coriander sativum* by applying a water saving tactic (water stress regimes) for the production of sustainable biomass and EY. Further, the acquisition of water stress tolerance in *Coriander sativum* could be the result of enhanced activities of antioxidant enzymes and high content of osmolytes at lower magnitudes of water stress, which increased resistance to oxidative stress and promotes the overall growth of plant. Detailed study of this complex phenomena of tolerance through NPs needs further research at a molecular level to explore the annotation of genes.

Author Contributions: M.T.K. planned the research work, executed it, data collection, statistical analysis; M.T.K. and A.A.S., writing paper; S.A. assisted in designing research plan and supervised the overall work. A.N.S., M.T., M.A.E.-S. assisted in writing and proof reading. Funding acquisition, M.H.S. All authors have read and agreed to the published version of the manuscript.

Funding: Researchers Supporting Project number (RSP-2021/347), King Saud University, Riyadh, Saudi Arabia.

Institutional Review Board Statement: Not applicable.

Informed Consent Statement: Not applicable.

Data Availability Statement: The data presented in this study are available on request from the corresponding author.

Acknowledgments: The authors would like to extend their sincere appreciation to the Research Supporting Project Number (RSP-2021/347), King Saud University, Riyadh, Saudi Arabia.

Conflicts of Interest: Authors have declared no conflict of interest.

References

1. Liang, X.-Z.; Wu, Y.; Chambers, R.G.; Schmoldt, D.L.; Gao, W.; Liu, C.; Liu, Y.-A.; Sun, C.; Kennedy, J.A. Determining climate effects on US total agricultural productivity. *Proc. Natl. Acad. Sci. USA* **2017**, *114*, E2285–E2292. [\[CrossRef\]](#)
2. Troy, T.J.; Kipgen, C.; Pal, I. The impact of climate extremes and irrigation on US crop yields. *Environ. Res. Lett.* **2015**, *10*, 054013. [\[CrossRef\]](#)
3. Karl, T.R.; Melillo, J.M.; Peterson, T.C.; Hassol, S.J. *Global Climate Change Impacts in the United States*; Cambridge University Press: Cambridge, UK, 2009.
4. Winter, J.M.; Lopez, J.R.; Ruane, A.C.; Young, C.A.; Scanlon, B.R.; Rosenzweig, C. Representing water scarcity in future agricultural assessments. *Anthropocene* **2017**, *18*, 15–26. [\[CrossRef\]](#)
5. Abdelkhalik, A.; Pascual, B.; Nájera, I.; Baixauli, C.; Pascual-Seva, N. Regulated deficit irrigation as a water-saving strategy for onion cultivation in Mediterranean conditions. *Agronomy* **2019**, *9*, 521. [\[CrossRef\]](#)
6. Kang, Y.; Khan, S.; Ma, X. Climate change impacts on crop yield, crop water productivity and food security—A review. *Prog. Nat. Sci.* **2009**, *19*, 1665–1674. [\[CrossRef\]](#)
7. Capra, A.; Consoli, S.; Scicolone, B. *Deficit Irrigation: Theory and Practice*; Nova Science Publishers: New York, NY, USA, 2008; pp. 53–82.
8. Wang, R.; Gao, M.; Ji, S.; Wang, S.; Meng, Y.; Zhou, Z. Carbon allocation, osmotic adjustment, antioxidant capacity and growth in cotton under long-term soil drought during flowering and boll-forming period. *Plant Physiol. Biochem.* **2016**, *107*, 137–146. [\[CrossRef\]](#)
9. Sriti, J.; Talou, T.; Wannes, W.A.; Cerny, M.; Marzouk, B. Essential oil, fatty acid and sterol composition of Tunisian coriander fruit different parts. *J. Sci. Food Agric.* **2009**, *89*, 1659–1664. [\[CrossRef\]](#)
10. Begnami, A.; Duarte, M.; Furletti, V.; Rehder, V. Antimicrobial potential of *Coriandrum sativum* L. against different *Candida* species in vitro. *Food Chem.* **2010**, *118*, 74–77. [\[CrossRef\]](#)
11. Ahmad, P.; Alyemeni, M.N.; AlHuqail, A.A.; Alqahtani, M.A.; Wijaya, L.; Ashraf, M.; Kaya, C.; Bajguz, A. Zinc Oxide Nanoparticles Application Alleviates Arsenic (As) Toxicity in Soybean Plants by Restricting the Uptake of as and Modulating Key Biochemical Attributes, Antioxidant Enzymes, Ascorbate-Glutathione Cycle and Glyoxalase System. *Plants* **2020**, *9*, 825. [\[CrossRef\]](#)
12. Shah, T.; Latif, S.; Saeed, F.; Ali, I.; Ullah, S.; Alsahli, A.A.; Jan, S.; Ahmad, P. Seed priming with titanium dioxide nanoparticles enhances seed vigor, leaf water status, and antioxidant enzyme activities in maize (*Zea mays* L.) under salinity stress. *J. King Saud Univ.—Sci.* **2021**, *33*, 101207. [\[CrossRef\]](#)
13. Lian, J.; Zhao, L.; Wu, J.; Xiong, H.; Bao, Y.; Zeb, A.; Tang, J.; Liu, W. Foliar spray of TiO₂ nanoparticles prevails over root application in reducing Cd accumulation and mitigating Cd-induced phytotoxicity in maize (*Zea mays* L.). *Chemosphere* **2020**, *239*, 124794. [\[CrossRef\]](#)
14. Lee, J.-S.; Wissuwa, M.; Zamora, O.B.; Ismail, A.M. Biochemical indicators of root damage in rice (*Oryza sativa*) genotypes under zinc deficiency stress. *J. Plant Res.* **2017**, *130*, 1071–1077. [\[CrossRef\]](#)
15. Ditta, A.; Arshad, M. Applications and perspectives of using nanomaterials for sustainable plant nutrition. *Nanotechnol. Rev.* **2016**, *5*, 209–229. [\[CrossRef\]](#)
16. Abbasifar, A.; Shahrabadi, F.; ValizadehKaji, B. Effects of green synthesized zinc and copper nano-fertilizers on the morphological and biochemical attributes of basil plant. *J. Plant Nutr.* **2020**, *43*, 1104–1118. [\[CrossRef\]](#)
17. Dimkpa, C.O.; Singh, U.; Bindraban, P.S.; Elmer, W.H.; Gardea-Torresdey, J.L.; White, J.C. Zinc oxide nanoparticles alleviate drought-induced alterations in sorghum performance, nutrient acquisition, and grain fortification. *Sci. Total Environ.* **2019**, *688*, 926–934. [\[CrossRef\]](#)
18. Rashwan, E.; Alsohim, A.S.; El-Gammaal, A.; Hafez, Y.; Abdelaal, K.A. Foliar application of nano zink-oxide can alleviate the harmful effects of water deficit on some flax cultivars under drought conditions. *Fresenius Environ. Bull.* **2020**, *29*, 8889–8904.
19. Korbekandi, H.; Iravani, S.; Abbasi, S. Production of nanoparticles using organisms. *Crit. Rev. Biotechnol.* **2009**, *29*, 279–306. [\[CrossRef\]](#)
20. Suresh, D.; Nethravathi, P.; Rajanaika, H.; Nagabhushana, H.; Sharma, S. Green synthesis of multifunctional zinc oxide (ZnO) nanoparticles using *Cassia fistula* plant extract and their photodegradative, antioxidant and antibacterial activities. *Mater. Sci. Semicond. Process.* **2015**, *31*, 446–454. [\[CrossRef\]](#)
21. Fakhari, S.; Jamzad, M.; Kabiri Fard, H. Green synthesis of zinc oxide nanoparticles: A comparison. *Green Chem. Lett. Rev.* **2019**, *12*, 19–24. [\[CrossRef\]](#)
22. Bala, N.; Saha, S.; Chakraborty, M.; Maiti, M.; Das, S.; Basu, R.; Nandy, P. Green synthesis of zinc oxide nanoparticles using *Hibiscus subdariffa* leaf extract: Effect of temperature on synthesis, anti-bacterial activity and anti-diabetic activity. *RSC Adv.* **2015**, *5*, 4993–5003. [\[CrossRef\]](#)
23. Samat, N.A.; Nor, R.M. Sol–gel synthesis of zinc oxide nanoparticles using *Citrus aurantifolia* extracts. *Ceram. Int.* **2013**, *39*, S545–S548. [\[CrossRef\]](#)
24. Demissie, M.G.; Sabir, F.K.; Edossa, G.D.; Gonfa, B.A. Synthesis of zinc oxide nanoparticles using leaf extract of lippia adoensis (koseret) and evaluation of its antibacterial activity. *J. Chem.* **2020**, *2020*. [\[CrossRef\]](#)
25. Rasli, N.I.; Basri, H.; Harun, Z. Zinc oxide from aloe vera extract: Two-level factorial screening of biosynthesis parameters. *Heliyon* **2020**, *6*, e03156. [\[CrossRef\]](#)

26. Elumalai, K.; Velmurugan, S.; Ravi, S.; Kathiravan, V.; Ashokkumar, S. *RETRACTED: Green Synthesis of Zinc Oxide Nanoparticles Using Moringa Oleifera Leaf Extract and Evaluation of Its Antimicrobial Activity*; Elsevier: Amsterdam, The Netherlands, 2015.
27. Ogunyemi, S.O.; Abdallah, Y.; Zhang, M.; Fouad, H.; Hong, X.; Ibrahim, E.; Masum, M.M.I.; Hossain, A.; Mo, J.; Li, B. Green synthesis of zinc oxide nanoparticles using different plant extracts and their antibacterial activity against *Xanthomonas oryzae* pv. *oryzae*. *Artif. Cells Nanomed. Biotechnol.* **2019**, *47*, 341–352. [\[CrossRef\]](#)
28. Hussain, A.; Ali, S.; Rizwan, M.; ur Rehman, M.Z.; Javed, M.R.; Imran, M.; Chatha, S.A.S.; Nazir, R. Zinc oxide nanoparticles alter the wheat physiological response and reduce the cadmium uptake by plants. *Environ. Pollut.* **2018**, *242*, 1518–1526. [\[CrossRef\]](#)
29. Zahedi, S.M.; Karimi, M.; Teixeira da Silva, J.A. The use of nanotechnology to increase quality and yield of fruit crops. *J. Sci. Food Agric.* **2020**, *100*, 25–31. [\[CrossRef\]](#)
30. Sun, L.; Song, F.; Guo, J.; Zhu, X.; Liu, S.; Liu, F.; Li, X. Nano-ZnO-induced drought tolerance is associated with melatonin synthesis and metabolism in maize. *Int. J. Mol. Sci.* **2020**, *21*, 782. [\[CrossRef\]](#) [\[PubMed\]](#)
31. Prasad, T.; Sudhakar, P.; Sreenivasulu, Y.; Latha, P.; Munaswamy, V.; Reddy, K.R.; Sreeprasad, T.; Sajanlal, P.; Pradeep, T. Effect of nanoscale zinc oxide particles on the germination, growth and yield of peanut. *J. Plant Nutr.* **2012**, *35*, 905–927. [\[CrossRef\]](#)
32. Singh, A.; Singh, N.; Hussain, I.; Singh, H.; Yadav, V.; Singh, S. Green synthesis of nano zinc oxide and evaluation of its impact on germination and metabolic activity of *Solanum lycopersicum*. *J. Biotechnol.* **2016**, *233*, 84–94. [\[CrossRef\]](#)
33. Mahajan, P.; Dhoke, S.; Khanna, A. Effect of nano-ZnO particle suspension on growth of mung (*Vigna radiata*) and gram (*Cicer arietinum*) seedlings using plant agar method. *J. Nanotechnol.* **2011**, *2011*, 696535. [\[CrossRef\]](#)
34. Adrees, M.; Khan, Z.S.; Hafeez, M.; Rizwan, M.; Hussain, K.; Asrar, M.; Alyemeni, M.N.; Wijaya, L.; Ali, S. Foliar exposure of zinc oxide nanoparticles improved the growth of wheat (*Triticum aestivum* L.) and decreased cadmium concentration in grains under simultaneous Cd and water deficient stress. *Ecotoxicol. Environ. Saf.* **2021**, *208*, 111627. [\[CrossRef\]](#) [\[PubMed\]](#)
35. Semida, W.M.; Abdelkhalik, A.; Mohamed, G.; El-Mageed, A.; Taia, A.; El-Mageed, A.; Shima, A.; Rady, M.M.; Ali, E.F. Foliar application of zinc oxide nanoparticles promotes drought stress tolerance in eggplant (*Solanum melongena* L.). *Plants* **2021**, *10*, 421. [\[CrossRef\]](#) [\[PubMed\]](#)
36. Senthilkumar, S.; Sivakumar, T. Green tea (*Camellia sinensis*) mediated synthesis of zinc oxide (ZnO) nanoparticles and studies on their antimicrobial activities. *Int. J. Pharm. Pharm. Sci.* **2014**, *6*, 461–465.
37. Hammerschmidt, R.; Nuckles, E.; Kuć, J. Association of enhanced peroxidase activity with induced systemic resistance of cucumber to *Colletotrichum lagenarium*. *Physiol. Plant Pathol.* **1982**, *20*, 73–82. [\[CrossRef\]](#)
38. Worthington, C.C. *Worthington Enzyme Manual: Enzymes and Related Biochemicals*; Worthington Biochemical Corporation: Lakewood, NJ, USA, 1988.
39. Weisany, W.; Sohrabi, Y.; Heidari, G.; Siosemardeh, A.; Ghassemi-Golezani, K. Changes in antioxidant enzymes activity and plant performance by salinity stress and zinc application in soybean (*Glycine max* L.). *Plant Omics* **2012**, *5*, 60–67.
40. Paoletti, F.; Aldinucci, D.; Mocali, A.; Caparrini, A. A sensitive spectrophotometric method for the determination of superoxide dismutase activity in tissue extracts. *Anal. Biochem.* **1986**, *154*, 536–541. [\[CrossRef\]](#)
41. McCord, J.M.; Fridovich, I. Superoxide dismutase: An enzymic function for erythrocuprein (hemocuprein). *J. Biol. Chem.* **1969**, *244*, 6049–6055. [\[CrossRef\]](#)
42. Zhang, C.; Bruins, M.E.; Yang, Z.Q.; Liu, S.T.; Rao, P.F. A new formula to calculate activity of superoxide dismutase in indirect assays. *Anal. Biochem.* **2016**, *503*, 65–67. [\[CrossRef\]](#)
43. Nakano, Y.; Asada, K. Purification of ascorbate peroxidase in spinach chloroplasts; its inactivation in ascorbate-depleted medium and reactivation by monodehydroascorbate radical. *Plant Cell Physiol.* **1987**, *28*, 131–140.
44. Arnon, D.I. Copper enzymes in isolated chloroplasts. Polyphenoloxidase in *Beta vulgaris*. *Plant Physiol.* **1949**, *24*, 1. [\[CrossRef\]](#) [\[PubMed\]](#)
45. Davies, B.; Goodwin, T. Chemistry and biochemistry of plant pigments. *Carotenoids* **1976**, *2*, 38–165.
46. Bates, L.S.; Waldren, R.P.; Teare, I. Rapid determination of free proline for water-stress studies. *Plant Soil* **1973**, *39*, 205–207. [\[CrossRef\]](#)
47. Zhao, F.; Guo, S.; Zhang, H.; Zhao, Y. Expression of yeast SOD2 in transgenic rice results in increased salt tolerance. *Plant Sci.* **2006**, *170*, 216–224. [\[CrossRef\]](#)
48. Daughtry, C.S. Direct measurements of canopy structure. *Remote Sens. Rev.* **1990**, *5*, 45–60. [\[CrossRef\]](#)
49. Donald, C.; Hamblin, J. The biological yield and harvest index of cereals as agronomic and plant breeding criteria. *Adv. Agron.* **1976**, *28*, 361–405.
50. Datta, A.; Patra, C.; Bharadwaj, H.; Kaur, S.; Dimri, N.; Khajuria, R. Green synthesis of zinc oxide nanoparticles using parthenium hysterophorus leaf extract and evaluation of their antibacterial properties. *J. Biotechnol. Biomater* **2017**, *7*, 271–276. [\[CrossRef\]](#)
51. Hassan, S.S.; El Azab, W.I.; Ali, H.R.; Mansour, M.S. Green synthesis and characterization of ZnO nanoparticles for photocatalytic degradation of anthracene. *Adv. Nat. Sci. Nanosci. Nanotechnol.* **2015**, *6*, 045012. [\[CrossRef\]](#)
52. Shah, R.K.; Boruah, F.; Parween, N. Synthesis and characterization of ZnO nanoparticles using leaf extract of *Camellia sinensis* and evaluation of their antimicrobial efficacy. *Int. J. Curr. Microbiol. App. Sci.* **2015**, *4*, 444–450.
53. Salman, S.; Kuroda, K.; Okido, M. Preparation and Characterization of Hydroxyapatite Coating on AZ31 Mg Alloy for Implant Applications. *Bioinorg. Chem. Appl.* **2013**, *2013*, 175756. [\[CrossRef\]](#) [\[PubMed\]](#)
54. Dobrucka, R.; Długaszeńska, J.; Kaczmarek, M. Cytotoxic and antimicrobial effects of biosynthesized ZnO nanoparticles using of *Chelidonium majus* extract. *Biomed. Microdevices* **2018**, *20*, 1–13. [\[CrossRef\]](#)

55. Selim, Y.A.; Azb, M.A.; Ragab, I.; Abd El-Azim, M.H. Green synthesis of zinc oxide nanoparticles using aqueous extract of *Deverra tortuosa* and their cytotoxic activities. *Sci. Rep.* **2020**, *10*, 1–9. [\[CrossRef\]](#)
56. Xaba, T.; Mongwai, P.P.; Lesaoana, M. Decomposition of bis (N-benzyl-salicydenaminato) zinc (II) complex for the synthesis of ZnO nanoparticles to fabricate ZnO-chitosan nanocomposite for the removal of iron (II) ions from wastewater. *J. Chem.* **2019**, *2019*, 1907083. [\[CrossRef\]](#)
57. Mahamuni, P.P.; Patil, P.M.; Dhanavade, M.J.; Badiger, M.V.; Shadija, P.G.; Lokhande, A.C.; Bohara, R.A. Synthesis and characterization of zinc oxide nanoparticles by using polyol chemistry for their antimicrobial and antibiofilm activity. *Biochem. Biophys. Rep.* **2019**, *17*, 71–80. [\[CrossRef\]](#) [\[PubMed\]](#)
58. Madhumitha, G.; Fowsiya, J.; Gupta, N.; Kumar, A.; Singh, M. Green synthesis, characterization and antifungal and photocatalytic activity of *Pithecellobium dulce* peel-mediated ZnO nanoparticles. *J. Phys. Chem. Solids* **2019**, *127*, 43–51. [\[CrossRef\]](#)
59. Faisal, S.; Jan, H.; Shah, S.A.; Shah, S.; Khan, A.; Akbar, M.T.; Rizwan, M.; Jan, F.; Wajidullah; Akhtar, N. Green synthesis of zinc oxide (ZnO) nanoparticles using aqueous fruit extracts of *Myristica fragrans*: Their characterizations and biological and environmental applications. *ACS Omega* **2021**, *6*, 9709–9722. [\[CrossRef\]](#)
60. Guilger-Casagrande, M.; Lima, R.D. Synthesis of silver nanoparticles mediated by fungi: A review. *Front. Bioeng. Biotechnol.* **2019**, *7*, 287. [\[CrossRef\]](#) [\[PubMed\]](#)
61. Vijayakumar, S.; Mahadevan, S.; Arulmozhi, P.; Sriram, S.; Praseetha, P. Green synthesis of zinc oxide nanoparticles using *Atalantia monophylla* leaf extracts: Characterization and antimicrobial analysis. *Mater. Sci. Semicond. Process.* **2018**, *82*, 39–45. [\[CrossRef\]](#)
62. Awwad, A.M.; Albiss, B.; Ahmad, A.L. Green synthesis, characterization and optical properties of zinc oxide nanosheets using *Olea europea* leaf extract. *Adv. Mater. Lett.* **2014**, *5*, 520–524. [\[CrossRef\]](#)
63. Al-Dhabi, N.A.; Valan Arasu, M. Environmentally-friendly green approach for the production of zinc oxide nanoparticles and their anti-fungal, ovicidal, and larvicidal properties. *Nanomaterials* **2018**, *8*, 500. [\[CrossRef\]](#)
64. Yuvakkumar, R.; Suresh, J.; Saravanakumar, B.; Nathanael, A.J.; Hong, S.I.; Rajendran, V. Rambutan peels promoted biomimetic synthesis of bioinspired zinc oxide nanochains for biomedical applications. *Spectrochim. Acta Part A Mol. Biomol. Spectrosc.* **2015**, *137*, 250–258. [\[CrossRef\]](#)
65. Pillai, A.M.; Sivasankarapillai, V.S.; Rahdar, A.; Joseph, J.; Sadeghfar, F.; Rajesh, K.; Kyzas, G.Z. Green synthesis and characterization of zinc oxide nanoparticles with antibacterial and antifungal activity. *J. Mol. Struct.* **2020**, *1211*, 128107. [\[CrossRef\]](#)
66. Modena, M.M.; Rühle, B.; Burg, T.P.; Wuttke, S. Nanoparticle Characterization: Nanoparticle Characterization: What to Measure?(Adv. Mater. 32/2019). *Adv. Mater.* **2019**, *31*, 1970226. [\[CrossRef\]](#)
67. Jan, H.; Shah, M.; Usman, H.; Khan, A.; Muhammad, Z.; Hano, C.; Abbasi, B.H. Biogenic synthesis and characterization of antimicrobial and anti-parasitic zinc oxide (ZnO) nanoparticles using aqueous extracts of the *Himalayan columbine* (*Aquilegia pubiflora*). *Front. Mater.* **2020**, *7*, 249. [\[CrossRef\]](#)
68. Awwad, A.M.; Amer, M.W.; Salem, N.M.; Abdeen, A.O. Green synthesis of zinc oxide nanoparticles (ZnO-NPs) using *Ailanthus altissima* fruit extracts and antibacterial activity. *Chem. Int.* **2020**, *6*, 151–159.
69. Laxa, M.; Liebthal, M.; Telman, W.; Chibani, K.; Dietz, K.-J. The role of the plant antioxidant system in drought tolerance. *Antioxidants* **2019**, *8*, 94. [\[CrossRef\]](#) [\[PubMed\]](#)
70. Hu, C.; Liu, X.; Li, X.; Zhao, Y. Evaluation of growth and biochemical indicators of *Salvinia natans* exposed to zinc oxide nanoparticles and zinc accumulation in plants. *Environ. Sci. Pollut. Res.* **2014**, *21*, 732–739. [\[CrossRef\]](#) [\[PubMed\]](#)
71. Priyanka, N.; Venkatachalam, P. Biofabricated zinc oxide nanoparticles coated with phycomolecules as novel micronutrient catalysts for stimulating plant growth of cotton. *Adv. Nat. Sci. Nanosci. Nanotechnol.* **2017**, *7*, 045018. [\[CrossRef\]](#)
72. Sharifi-Rad, R.; Bahabadi, S.E.; Samzadeh-Kermani, A.; Gholami, M. The Effect of Non-biological Elicitors on Physiological and Biochemical Properties of Medicinal Plant *Momordica charantia* L. Iran. *J. Sci. Technol. Trans. A Sci.* **2020**, *44*, 1315–1326. [\[CrossRef\]](#)
73. Gurmani, A.R.; Khan, S.U.; Andaleep, R.; Waseem, K.; Khan, A. Soil application of zinc improves growth and yield of tomato. *Int. J. Agric. Biol.* **2012**, *14*, 91–96.
74. Latef, A.A.H.A.; Alhmad, M.F.A.; Abdelfattah, K.E. The possible roles of priming with ZnO nanoparticles in mitigation of salinity stress in lupine (*Lupinus termis*) plants. *J. Plant Growth Regul.* **2017**, *36*, 60–70. [\[CrossRef\]](#)
75. Priester, J.H.; Moritz, S.C.; Espinosa, K.; Ge, Y.; Wang, Y.; Nisbet, R.M.; Schimel, J.P.; Goggi, A.S.; Gardea-Torresdey, J.L.; Holden, P.A. Damage assessment for soybean cultivated in soil with either CeO₂ or ZnO manufactured nanomaterials. *Sci. Total Environ.* **2017**, *579*, 1756–1768. [\[CrossRef\]](#) [\[PubMed\]](#)
76. Ahmad, P.; Jaleel, C.A.; Salem, M.A.; Nabi, G.; Sharma, S. Roles of enzymatic and nonenzymatic antioxidants in plants during abiotic stress. *Crit. Rev. Biotechnol.* **2010**, *30*, 161–175. [\[CrossRef\]](#) [\[PubMed\]](#)
77. Ahmad, P.; Tripathi, D.K.; Deshmukh, R.; Singh, V.P.; Corpas, F.J. Revisiting the role of ROS and RNS in plants under changing environment. *Environ. Exp. Bot.* **2019**, *161*, 1–3. [\[CrossRef\]](#)
78. Kohli, S.K.; Khanna, K.; Bhardwaj, R.; Abde Allaha, E.; Ahmad, P.; Corpas, F.J. Assessment of Subcellular ROS and NO Metabolism in Higher Plants: Multifunctional Signaling Molecules. *Antioxidants* **2019**, *8*, 641. [\[CrossRef\]](#)
79. Tiwari, S.; Lata, C.; Chauhan, P.S.; Nautiyal, C.S. *Pseudomonas putida* attunes morphophysiological, biochemical and molecular responses in *Cicer arietinum* L. during drought stress and recovery. *Plant Physiol. Biochem.* **2016**, *99*, 108–117. [\[CrossRef\]](#)
80. Mushtaq, T.; Hussain, S.; Bukhsh, M.; Iqbal, J.; Khaliq, T. Evaluation of two wheat genotypes performance of under drought conditions at different growth stages. *Crop Environ.* **2011**, *2*, 20–27.

81. Memon, S.A.; Sheikh, I.A.; Talpur, M.A.; Mangrio, M.A. Impact of deficit irrigation strategies on winter wheat in semi-arid climate of sindh. *Agric. Water Manag.* **2021**, *243*, 106389. [[CrossRef](#)]
82. Ibrahim, M.; Ibrahim, H.A.; Abd El-Gawad, H. Folic acid as a protective agent in snap bean plants under water deficit conditions. *J. Hortic. Sci. Biotechnol.* **2021**, *96*, 94–109. [[CrossRef](#)]
83. Gholizadeh, A.; Dehghani, H.; Khodadadi, M.; Gulick, P.J. Genetic combining ability of coriander genotypes for agronomic and phytochemical traits in response to contrasting irrigation regimes. *PLoS ONE* **2018**, *13*, e0199630. [[CrossRef](#)]
84. Manuchehri, R.; Salehi, H. Physiological and biochemical changes of common bermudagrass (*Cynodon dactylon* [L.] Pers.) under combined salinity and deficit irrigation stresses. *S. Afr. J. Bot.* **2014**, *92*, 83–88. [[CrossRef](#)]
85. Waqas, M.A.; Kaya, C.; Riaz, A.; Farooq, M.; Nawaz, I.; Wilkes, A.; Li, Y. Potential mechanisms of abiotic stress tolerance in crop plants induced by thiourea. *Front. Plant Sci.* **2019**, *10*, 1336. [[CrossRef](#)]
86. Pour-Aboughadareh, A.; Ahmadi, J.; Mehrabi, A.A.; Etminan, A.; Moghaddam, M.; Siddique, K.H. Physiological responses to drought stress in wild relatives of wheat: Implications for wheat improvement. *Acta Physiol. Plant.* **2017**, *39*, 106. [[CrossRef](#)]
87. Pour-Aboughadareh, A.; Omid, M.; Naghavi, M.R.; Etminan, A.; Mehrabi, A.A.; Pocza, P.; Bayat, H. Effect of water deficit stress on seedling biomass and physio-chemical characteristics in different species of wheat possessing the D genome. *Agronomy* **2019**, *9*, 522. [[CrossRef](#)]
88. Jakobsson, A.; Eriksson, O. A comparative study of seed number, seed size, seedling size and recruitment in grassland plants. *Oikos* **2000**, *88*, 494–502. [[CrossRef](#)]
89. Iglesias, F.M.; Miralles, D.J. Changes in seed weight in response to different sources: Sink ratio in oilseed rape. *Int. J. Agric. Res. Innov. Technol.* **2014**, *4*, 44–52. [[CrossRef](#)]
90. Smith, M.R.; Rao, I.M.; Merchant, A. Source-sink relationships in crop plants and their influence on yield development and nutritional quality. *Front. Plant Sci.* **2018**, *9*, 1889. [[CrossRef](#)]
91. Sah, R.; Chakraborty, M.; Prasad, K.; Pandit, M.; Tudu, V.; Chakravarty, M.; Narayan, S.; Rana, M.; Moharana, D. Impact of water deficit stress in maize: Phenology and yield components. *Sci. Rep.* **2020**, *10*, 1–15. [[CrossRef](#)]
92. Jacques, M.M.; Gumiere, S.J.; Gallichand, J.; Celicourt, P.; Gumiere, T. Impacts of water stress severity and duration on potato photosynthetic activity and yields. *Front. Agron.* **2020**, *2*, 19. [[CrossRef](#)]
93. Hatfield, J.L.; Dold, C. Water-use efficiency: Advances and challenges in a changing climate. *Front. Plant Sci.* **2019**, *10*, 103. [[CrossRef](#)]
94. Seleiman, M.F.; Al-Suhaibani, N.; Ali, N.; Akmal, M.; Alotaibi, M.; Refay, Y.; Dindaroglu, T.; Abdul-Wajid, H.H.; Battaglia, M.L. Drought stress impacts on plants and different approaches to alleviate its adverse effects. *Plants* **2021**, *10*, 259. [[CrossRef](#)]
95. Sun, L.; Song, F.; Zhu, X.; Liu, S.; Liu, F.; Wang, Y.; Li, X. Nano-ZnO alleviates drought stress via modulating the plant water use and carbohydrate metabolism in maize. *Arch. Agron. Soil Sci.* **2021**, *67*, 245–259. [[CrossRef](#)]
96. Dhoke, S.K.; Mahajan, P.; Kamble, R.; Khanna, A. Effect of nanoparticles suspension on the growth of mung (*Vigna radiata*) seedlings by foliar spray method. *Nanotechnol. Dev.* **2013**, *3*, e1. [[CrossRef](#)]
97. Alabdallah, N.M.; Hasan, M.; Hammami, I.; Alghamdi, A.I.; Alshehri, D.; Alatawi, H.A. Green Synthesized Metal Oxide Nanoparticles Mediate Growth Regulation and Physiology of Crop Plants under Drought Stress. *Plants* **2021**, *10*, 1730. [[CrossRef](#)] [[PubMed](#)]
98. Ghasemi, M.; Ghorban, N.; Madani, H.; Mobasser, H.R.; Nouri, M.Z. Effect of foliar application of zinc nano oxide on agronomic traits of two varieties of rice (*Oryza sativa* L.). *Crop Res.* **2017**, *52*, 195–201. [[CrossRef](#)]